Identification of the Anisotropic Elastic and Damping Properties of Complex Shape Composite Parts Using an Inverse...

Article · December 2017

DOI: 10.1016/j.compositesa.2017.12.018

CITATIONS
0

READS
25

3 authors:

Romain Viala
Institut FEMTO-ST
16 PUBLICATIONS **0** CITATIONS
SEE PROFILE

Vincent Placet
University of Franche-Comté
104 PUBLICATIONS **636** CITATIONS
SEE PROFILE

Scott Cogan
University of Franche-Comté
160 PUBLICATIONS **538** CITATIONS
SEE PROFILE

Identification of the anisotropic elastic and damping properties of complex shape composite parts using an inverse method based on finite element model updating and 3D velocity fields measurements (FEMU-3DVF): Application to bio-based composite violin soundboards

Romain Viala[a], Vincent Placet[a], Scott Cogan[a]

[a] *Univ. Bourgogne Franche-Comté, FEMTO-ST Institute, CNRS/UFC/ENSMM/UTBM*
Department of Applied Mechanics, 25000 BESANÇON-FR, Tel.: +(33 3)81666010

Abstract

Inverse methods have been used for decades to identify material properties, in parallel, or as a substitution for direct methods. Although it has proven a useful method for many types of materials and simple geometrical shapes, it has barely been used on complex shape parts. This is the main objective of the non-destructive method proposed in this study. The proposed inverse approach, based on both vibrational experiment data and Finite Element Model Updating (FEMU), is successfully applied to a violin soundboard made of flax-epoxy composite. Results show that, by minimizing the discrepancy between the experimental and numerical data, three rigidities and three loss factors can be determined simultaneously. The identified values of the constitutive elastic moduli and longitudinal loss factor are in agreement with those determined using quasi-static tests and dynamic mechanical analysis.

Keywords: Non-destructive testing, Biocomposite, Mechanical properties, Finite element analysis

1. Introduction

As the utilization of composite materials in research and industry has been continuously growing over the last three decades, numerous identification methods have been developed to identify the material properties of composite parts. The wide variety of shapes and applications of composite materials has driven to more and more sophisticated manufacturing processes and characterization methods. Both direct and indirect methods are classically used. Direct methods estimate the material properties from experimental data and fundamental mechanics theories. The second ones, also called inverse methods, are based both on experiments and models and a minimization procedure for the identification of the parameters. Each method has its advantages and drawbacks and some are not necessarily adapted to complex shapes and complex constitutive behaviour. Direct methods are generally destructive or at least with contact and have been traditionally used to measure the properties of a wide variety of materials. They are still considered as reference methods for the study of new materials and can be used to evaluate material properties even when they exhibit a complex behaviour, such as composites [1]. The growing need for contact free methods for material characterization has led to the use of powerful experimental techniques, such as full-field measurements [2, 3] and resonant ultra-sonic methods [4, 5]. Some studies have successfully compared the results collected with such techniques to the ones obtained with standard static tests [6] and emphasized their capability and efficiency. Inverse methods based on both dynamic experimental data and Finite Element Model Updating (FEMU) can also be considered as a powerful method. The fitting of a numerical simulation with experiments using minimization methods [7] enables the determination of the properties of materials exhibiting a complex behaviour. This type of method is non-invasive, fast and easy to set-up. It requires a reduced preparation of the samples, compared to other traditional methods that require calibrated specimens. Moreover, dynamical responses, for example vibratory modes, are more representative of the global behaviour of the material when compared to static properties that are generally driven by local phenomena. These benefits have led to the development of numerically based identification methods over the last thirty years [8], as well as analytically based methods, to estimate both anisotropic loss factors and rigidities of composite plates [9]. The efficiency of the FEMU method in the case of non-standard specimen shapes has been assessed studying layered materials, and the impact of the grain angle on the material properties [10]. Sandwich structures have also been characterized using this validated method [11, 12, 13]. Many studies were focused on other types of structures or materials, like wooden beams [14], printed electric circuit material [15] and tonewood plates undergoing moisture content changes [16]. Only few studies concern different shapes, such as composite tubes [17]. More recently, in 2016, a review paper [18] made a list of the numerous works about the identification of material properties using vibrational approaches. This paper highlights

☆

Email address: romain.viala@univ-fcomte.fr ()

the fact that, despite its potential, this method has mostly been applied to flat plate specimens and not complex shape parts. These parts, such as silicon carbide blades or composite corner reinforcements, are generally made of materials whose properties depend on the manufacturing process. The indirect methods deal with uncertainties, and stochastic methods for model updating have been proposed in [19, 20] to quantify the sources of uncertainties due to the method. Nevertheless, stochastic methods need a large amount of experimental data and computations. As a conclusion of these different works, one remaining need is to use and validate FEMU method for 3D complex shaped parts which is the main purpose of this work. This study will focus on complex shapes and material behaviour to assess the efficiency of this method. The FEMU-3DVF method deals with a finite elements model and an experimental set-up constituted of an acoustic exciter (speaker) and a Doppler effect laser 3D vibrometer. This allows the determination, through the measurement of velocities at the surface of the specimen in the three material directions, of the dynamical response (operational modes) of the parts. The experimental data obtained are rich and detailed. The diversity of the resulting displacement fields of the specimen activate in a single experiment different material properties. The identification process requires an efficient method. This consists of the minimization of the discrepancies of the frequencies of the matched test-analysis modes. A preliminary sensitivity analysis is performed to determine which components of the compliance matrix of the constitutive law can be identified reliably, based on their influence on the computed modal basis. The parts studied in this work are half scale violin soundboards. Similar full-scale bio-based composite sandwiches made of flax fibre composite skins with a balsa core have been made as a substitute for bulk wood in the manufacturing of violin soundboard [21]. The bio-based composites are considered as an alternative to wood for the making of violin soundboard (spruce, *Picea abies*) [22]. The flax-epoxy composites show a lower variability than wood, and the cost of the materials used for bio-based composite soundboards is smaller than the cost of high quality tonewood. The sensitivity to relative humidity is also lower than for wood and thus it enhances the stability of musical instruments when undergoing climatic changes. Moreover, the loss factors of bio-based composite in the different material directions are closer to wood than glass or carbon fibre composites. Composite parts of violins are currently manufactured and studied, and the need of non-destructive characterization method is at the origin of the development of the FEMU-3DVF method. So, in this work, the capacity and performance of the proposed method is demonstrated at the scale of a violin soundboard made of bio-based composite, but the method is suitable for any given part with a complex 3D shape. In the following, the materials and methods used are fully described. The elastic and damping properties determined using FEMU-3DVF in the vibratory domain are compared to those obtained with quasi-static flexural tests and Dynamic Mechanical Analysis (DMA). A master curve built using DMA is used to compare the material properties at the same frequencies of solicitation that are used for the FEMU-3DVF method.

2. Materials and methods

2.1. Materials

The parts considered in this study are bio-based composite violin soundboards whose dimensions are half scale compared to standard sized soundboards. The soundboard of a violin is the top part of the body. It is traditionally hand carved to create an arch, and two f-shaped holes are cut symmetrically.

2.1.1. Composite violin soundboard manufacturing

The bio-based composite soundboards are manufactured by thermocompression of the flaxpreg T-UD® material, a pre-impregnated flaxtape provided by LINEO®. The areal weight of the reinforcements is 110 g/m^2. The resin that is used is the XB3515® and the hardener is the Aradur5021®. The manufacturing method is schematically represented in Fig. 1 (a). The parts are made of sixteen flax layers aligned and stacked. The layers are compressed in a Teflon coated aluminum mould and cured for one hour and a half at the cure temperature of 130 °C. The mould is machined to the shape of the arch of the violin soundboards using a numerical control machine and computer aided design. A pressure equal to 3 bars is applied for a period of 1 h after 30 min of heating. The arched plate is cut using a Trotec Speed300® laser device. The bio-based composite violin soundboard is represented in Fig. 1 (b).

Two soundboards (called S_1 and S_2) were made, their dimensions are determined manually with a sliding calliper for length, width and thickness of the edges. A compass calliper is used to measure the inner thickness of the part. Their lengths, from bottom to top of the soundboards are 167±0.05 mm. Their width, from left to right side on the lower part of the soundboard are 100±0.05 mm. The thicknesses have been measured at twenty points and the mean value is taken for the making of the model. The fibre mass fraction of the composite material, M_{fibre}, is calculated using eq. 1, with M_s the areal weight of the fibre reinforcement, N the number of layers, S the surface of one layer in the part and m, the mass of the sample.

$$M_{fibre} = \frac{N \times M_s \times S}{m} \tag{1}$$

The fibre volume fraction V_{fibre} is calculated using eq. 2, $\rho_{composite}$ represents the specific gravity of the composite. The value of the specific gravity of the fibre, ρ_{fibre}, is taken from [23] and is equal to 1.45.

$$V_{fibre} = \frac{M_{fibre} \times \rho_{composite}}{\rho_{fibre}} \tag{2}$$

The matrix volume fraction V_{matrix} is calculated following eq.3. The specific gravity of the matrix, ρ_{matrix}, is provided by the supplier and is equal to 1.15.

$$V_{matrix} = \frac{M_{matrix} \times \rho_{composite}}{\rho_{matrix}} \tag{3}$$

The porosity is calculated using eq. 4 :

$$V_{poro} = 1 - V_{matrix} - V_{fibre} \tag{4}$$

Figure 1: Composite soundboard, (a): Manufacturing tool scheme, (b): specimen and material orientation.

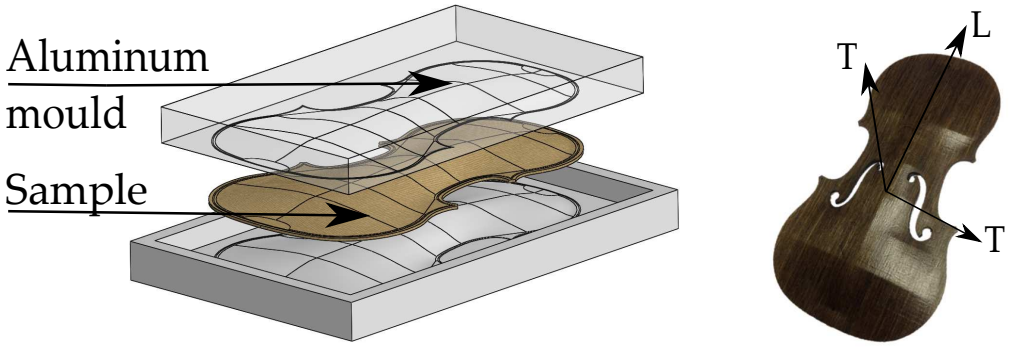

(a) (b)

The elastic moduli are evaluated using the rule of mixture (ROM). Equations 5 and 6 are used for the calculation of the theoretical elastic moduli values in longitudinal and transverse directions ($E_{L_{ROM}}$ and $E_{T_{ROM}}$, respectively).

$$E_{L_{ROM}} = E_f^L \times V_{fibre} + E_m \times V_{matrix} \tag{5}$$

$$\frac{1}{E_{T_{ROM}}} = \frac{1 - V_{fibre} - V_{porosity}}{E_m} + \frac{V_{fibre}}{E_f^T} \tag{6}$$

E_m corresponds to the elastic modulus of the matrix. According to the supplier data-sheet its value is equal to 3.5 GPa . E_f^L and E_f^T correspond to the stiffness of the fibre in longitudinal direction L and transverse direction T. For flax fibres, the average value of the longitudinal modulus is generally considered to be equal to approximately 60 GPa [24]. The transverse stiffness of an individual flax fibre, E_f^T, is generally considered to be 7 to 10 times lower than the longitudinal stiffness of the fibre [25], E_f^L. In this work, it was considered to be equal to 7 GPa. The specific gravity of the specimens was determined using the ratio between the measured mass and volume of the samples. The mass is measured using a KERN® 770 balance. The precision of the weighing scale is 0.1 mg. The volume was measured using the Archimedes' principle. The immersion time was short in order to avoid moisture sorption in the composite material during the measure.

2.1.2. Coupons for quasi-static tests and DMA

The samples for quasi static tests and Dynamical Mechanical Analysis (DMA) are cut from the remaining flat parts of the arched plates used to make flax fibre composite soundboards. They are laser cut in the longitudinal (L) and transverse (T) directions of the uni-directional composite. Their length, width and thickness are equal to 70, 45 and 2 mm, respectively.

2.2. FEMU-3DVF method description

In this section, the method used is indicated by the flow chart in Fig. 2, which shows the two main parts: the experimental set-up and the numerical model. In the identification process, computed eigenmodes of the structures are compared to experimentally measured operational modes.

Figure 2: FEMU-3DVF method. Representation of the iterative Scheme.

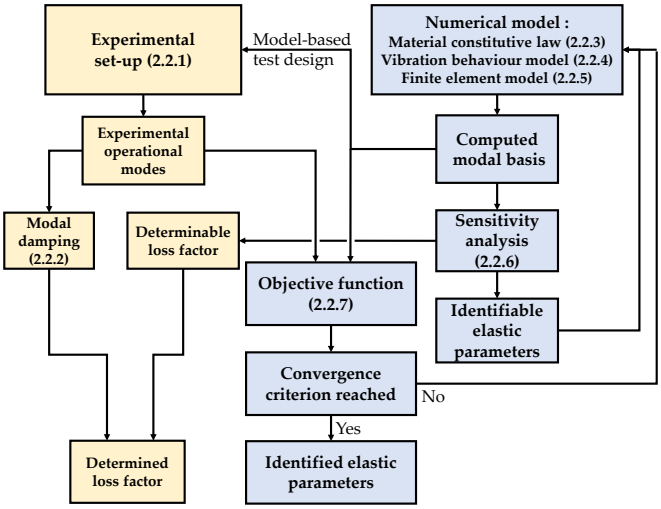

2.2.1. Experimental set-up

The experimental set-up is shown in Fig. 3.

Figure 3: Experimental set-up for 3D velocity field measurements on a composite part submitted to vibrational excitation.

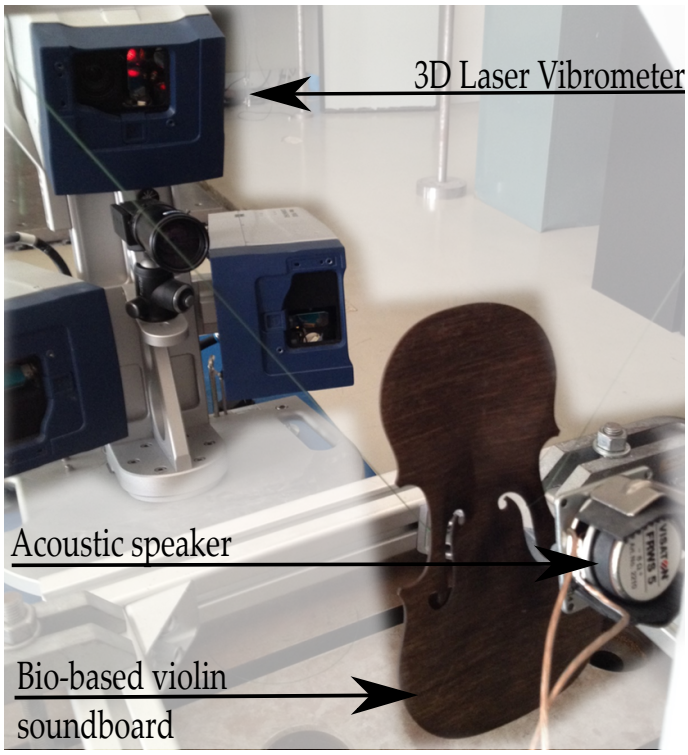

Measurements are made using a PSV-500 scanning laser 3D vibrometer from POLYTEC®, with a minimum resolution of 10 nm per second per square root of frequency, and the diameter of the measurement dot is close to 100 µm. The vibrometer performs local measurements on each predefined point and the fields are built by post-processing the relative velocities along each measured direction in the three main directions. A sweep sine excitation is performed between 150 and 3125 Hz and the frequency resolution is equal to 0.5 Hz. The sample is suspended by nylon threads knotted on each side of the f-holes, thus the boundary conditions are free-free. The number and location of the measurement points correspond to the nodes at the surface of the part of the numerical model detailed in 2.2.5. For the considered violin soudboard, it represents approximately 800 measurement points. The laser scan time lasts approximately thirty minutes according to the number of points measured and the precision of the sampling. The excitation, contact-free, is applied by a MONACOR® loudspeaker on a specific location of the studied structure, as indicated in [26]. The experimental configuration is designed and optimized using the model described in 2.2.5 and F.E. simulations. The properties provided by the material supplier and previous studies were considered at first. The excitation point location is specified using an excitability criterion of the different eigenmodes at this driving point. The distance between the part and the loudspeaker is 10 mm. An excitation tension of 1 V is applied at the output generator. The loudspeaker is amplified and the gain value is tuned to satisfy the coherence criterion, which is described below. The excitation is applied on the bottom left corner of the soundboard. The transfer function estimator that is used corresponds to the ratio between the interspectra output and the autospectra input. The autospectra corresponds to the Fourier transformation of the autocorrelation function. The interspectra is given by the Fourier transformation of the intercorrelation function. The coherence function ensures that the measured signal is in balance with the excitation. This indicator, ranging between 0 and 1 decreases with the noise level of the measured signal. The 3D velocity fields are used to estimate the modal basis. An in-house numerical tool developed using MATLAB® is used for the identification of the eigenmodes, based on the least square complex frequency (LSCF) method, with a phase shift criterion. The damping ratio is used to evaluate the loss factor of the material in the different directions. The loss factor can be calculated using the damping ratio in the case of a homogeneous structure and material, with the hypothesis that only one material direction is loaded. The 3D laser vibrometry also enables the evaluation of the full strain field tensor in the specimen for each measured mode. The sensitivity of the device allows the measurement of nano-strains. Throughout the study, the acoustic excitation on the considered parts leads to maximum measured strains of 50 n_ε, and 100 n_{rad} in the case of shear strains.

2.2.2. Loss factor determination

The modal damping ζ corresponding to each mode is calculated as a ratio between the imaginary and real parts of each eigenfrequency evaluated by least square complex frequency method. The loss factor η is determined using eq. 7 [27].

$$\eta = 2 \times \zeta \tag{7}$$

The results of the sensitivity analysis (see Section 2.2.6) are used to select the modes which are dominated mainly by the properties in a given material direction, such as pure torsion of bending modes. Thus, the loss factors η_L, η_T and η_{LT} are determined using the modal damping of the modes 5, 2 and 1, respectively (see Fig. 9). The modal damping value is given with an error of $\pm$ 0.001 , thus, the loss factors are given with an error of $\pm$ 0.002.

2.2.3. Material constitutive law

The material used to manufacture the violin soundboard is modelled based on macroscopic considerations with a continuum mechanics formulation. The bio-based composite exhibits heterogeneities at a microscopic scale. It is composed of fibre bundles embedded in an epoxy resin. For this study, focused at a macroscopic scale, it is considered as a homogeneous orthotropic material. Given the small level of strains applied, the hypothesis of small perturbations is assumed. Previous numerical simulations made with COMSOL® showed that for a damping capacity that is generally lower than 2.5%, the damping does not significantly influences the values of the eigenfrequencies. The relative variation of eigenfrequency values between damped and undamped simulations is less than 0.05% for frequencies ranging between 100 and 2000 Hz. For this reason, the

damping capacity was neglected in the model. Of course, the damping influences the amplitude of resonance peaks, but only the frequency is considered in the minimization process. Moreover, the computation of a modal basis is less time-consuming than a direct analysis that takes into account the damping and requieres calculations for each frequency step. Considering the small impact of the viscoelasticity, a linear elastic behaviour is used.

The compliance matrix $[S]$ depends on the elastic characteristic of the considered material. Based on the material symmetries, the elastic behaviour of an orthotropic material is completely defined by nine independent parameters (E_1, E_2, E_3, G_{12}, G_{23}, G_{31}, ν_{12}, ν_{23}, ν_{31}). The orthotropic compliance tensor $[S]_{ortho}$ is given in equation 8. In the following, E_i represents Young's modulus in i direction, ν_{ij} Poisson's ratios for i, j directions and G_{ij} shear modulus in i, j plane. The generalized form of the compliance matrix, for a material with three axes of symmetry is given by:

$$[S]_{ortho} = \begin{bmatrix} \frac{1}{E_1} & \frac{-\nu_{12}}{E_1} & \frac{-\nu_{13}}{E_1} & & & \\ \frac{-\nu_{21}}{E_2} & \frac{1}{E_2} & \frac{-\nu_{23}}{E_2} & & 0 & \\ \frac{-\nu_{31}}{E_3} & \frac{-\nu_{32}}{E_3} & \frac{1}{E_3} & & & \\ & & & \frac{1}{G_{23}} & & \\ & 0 & & & \frac{1}{G_{31}} & \\ & & & & & \frac{1}{G_{12}} \end{bmatrix}. \quad (8)$$

The orthotropic formulation corresponds to the general case. In the case of the UD composite tested in this work, the elastic properties in the transverse directions 2 and 3 are generally considered as similar. So, for the material properties a transversely isotropic assumption is made for the 2 and 3 directions. The numbering is related to material direction with 1: longitudinal direction (L) and 2,3: transverse direction (T).

2.2.4. Vibratory behaviour model

The experimental set-up is modelled as an undamped elastodynamic system model described under free-free boundary conditions. The forced response of the system is expressed by:

$$[M]\{\ddot{x}(t)\} + [K]\{x(t)\} = \{f(t)\} \quad (9)$$

[M] represents the mass matrix, and [K] the stiffness matrix. $\ddot{x}(t)$ and $x(t)$ are respectively the time dependent vectors of acceleration and displacement, and $f(t)$ the time dependent force vector. In the frequency domain, the equation of motion becomes:

$$\left[-\omega^2[M] + [K]\right]\{X(\omega)\} = \{F(\omega)\} \quad (10)$$

where ω represents the angular frequency, $\{X(\omega)\}$ the frequency dependent displacement vector, and $\{F(\omega)\}$ the force vector in frequency domain. The associated homogeneous equation under free vibrations is:

$$[K][\Phi] = [M][\Phi][\Lambda] \quad (11)$$

in this equation, $[\Lambda]$ corresponds to the diagonal eigenvalue matrix and $[\Phi]$ is the eigenvector matrix.

2.2.5. Finite element model

The geometry of the soundboards is built using the computer-aided design software SOLIDWORKS®. The geometry is exported in the parasolid format to the finite element software MSC-PATRAN®. This pre-processor generates the FE mesh and defines the material properties. Tetrahedral elements with quadratic interpolation (TET10) are used to mesh the structure and the mesh size is adapted to balance computation time and mesh convergence. The standard mesh convergence criterion is used leading to a mesh density of at least six quadratic elements per wavelength. The number of degrees of freedom is approximatively 100,000. A personal computer with a quad-core CPU and 8 Go of RAM is used in this study. The overall CPU time is approximatively two minutes. The solver software used is MSC-NASTRAN®, and the eigenvalue extraction method used is block Lanczos. These steps lead to the computation of eigenmodes of the undamped modal solution of the system, with eigenfrequencies and eigenvectors as the outputs.

2.2.6. Sensitivity analysis

A sensitivity analysis was performed with both the Morris method [28] and finite differences sensitivity method to rank the parameters sensitivities and determine the different material properties that can be identified for the considered composite soundboard. The output features of interest are the matched eigenfrequencies. At the end of the finite difference sensitivity analysis, the cartography of each parameter effect on the matched eigenfrequencies and eigenvectors of each mode is obtained, arranged in a sensitivity matrix, giving material parameters as a function of the mode number. This method evaluates the sensitivity of each parameter by applying a relative variation on its value of 1 %. This method is not sufficient to explore the complete parameter space, and so the Morris method is used. Four different levels and twenty trajectories are defined to explore the material parameter space. Nominal values are taken from the literature for similar materials, as well as their range of distribution. The objective function of the sensitivity analysis defined is the sum of the errors of all matched eigenfrequencies between model and experimental data. The experimental points are paired with the nodes of the numerical model using a geometric criterion: the closest nodes and points are paired. The mode matching is based on modal assurance criterion [29] which leads to a matrix whose components values are normalized between 0 and 1, with 1 indicating the test-analysis modes are affine and 0 indicating they are orthogonal. If two eigen bases are identical, the MAC matrix is an identity matrix. The modes are considered matched when the MAC value is above 0.7. Once the influential material parameters are identified, the remaining non influential parameters are fixed at their nominal values and the model updating procedure is applied uniquely on the influential ones.

2.2.7. Parameters identification

In this study, a deterministic model updating method has been chosen to estimate the material properties of the soundboards based on the available experimental data. This choice is coherent with the overall objective of this work which is to

obtain an optimal estimation for a specific and generally unique material specimen, and not a statistical model for a population of nominally identical soundboards. In the later case, variance correction or Bayesian methods would have been more relevant. The model updating approach used in this study is iterative in nature and is fully described in [7]. A test-analysis metric based on the discrepancy between a set of matched measured and simulated eigenfrequencies is constructed by expressing this difference as a product of the first-order sensitivity matrix of each eigenfrequency, calculated with respect to the parameters to be identified, and the corresponding parameter variations. This approach assumes that the experimental eigenmodes can be systematically and uniquely matched to the homologous analysis modes at each iteration. Convergence is obtained when the least-squared eigenfrequency error stabilizes over several successive iterations.

The parameters of the constitutive behaviour law are identified by minimizing the discrepancy between the experimental and the simulated data using an optimization procedure. The optimization is performed using a deterministic first order sensitivity method based on the matched eigenfrequencies.

2.3. Dynamic Mechanical Analysis and quasi-static tests

Quasi-static tests and Dynamic Mechanical Analysis (DMA) were performed on an electro-dynamical device BOSE electroforce®3230. The specimens are cut from the same plates as the soundboards, in the flat areas. A total of six specimens are cut. Three correspond to the longitudinal direction and three to the transverse direction. The specimens are tested by using a three point bending test. The distance between the supports is 45 mm. For the quasi-static test, displacement is applied at a rate of 40 µm/s. The load cell capacity is 450 N. The apparent moduli at 0 % strain in the longitudinal and transverse directions, $E^0_{L_{exp}}$ and $E^0_{T_{exp}}$ are calculated using the tangent method. For the dynamical mechanical analysis tests, a dynamic force that ranges between 0.5 and 1.5 N is applied on the sample at different frequencies (varying between 0.1 and 10 Hz). The temperature sweep band is in a range between -40 °C and 175 °C with 5 °C steps held during one minute. The heating rate is 0.1 °C.s^{-1}. The post-processing of the results is made using MATLAB® algorithms. The dynamical mechanical analysis of the longitudinal sample yields an estimation of the longitudinal storage modulus $E_{L_{DMA}}$, and loss factor $\eta_{L_{DMA}}$. A time-temperature superposition is built using DMA analysis. This method considers that a change in temperature from T_{ref} to T is analogous to multiplying the time scale by a constant factor aT. The post-processing method used to obtain the shift factors aT is taken from [30]. In this case, the shift factors are obtained through an optimization procedure (least square technique) for a reference temperature T_{ref} selected arbitrarily. The reference temperature T_{ref} for the master curve is 24 °C.

2.4. Error quantification

Three sources of error are considered. The first one is the error made on the specific gravity evaluation. The absolute error of the specific gravity is equal to 0.005, which leads to a relative error on the specific gravity evaluation of ±0.5 %. The second source of error is the measurement of the dimensions, and especially the thickness. The absolute error of the thickness is 0.05 mm, which leads to a relative error close to ±2.5 %. The values of thickness and density corresponding to the lower and upper bounds of the physical parameters measured are implemented in the numerical model. The propagation of these errors is evaluated with the shift of the predicted frequencies and the changes in the identified values for each cases separately. Finally, an error quantification method is used to evaluate the error that is due to the minimization method. For this purpose, a metamodel of the matched eigenfrequencies corresponding to the sample S_1 is used. The metamodel is created with a polynomial response surface of the third degree. A full factorial sampling of the parameter values, ranging between 30 and 50 GPa for E_L, 3.5 and 5 GPa for E_T and 1.5 and 3 GPa for G_{LT}, is performed. The design space is divided into 50 samples for each parameter. The cost function is defined as the sum of the matched eigenfrequencies error. It is calculated for each point in the design space. In total, 125,000 computations are performed using the metamodel. The minimum value of the cost function is represented by a 3D contour. The evaluation of the error on the identified values of the algorithm is based on the evaluation of the minimum and maximum values of each parameter, gathered in sets of equivalent values of the cost function.

3. Results

3.1. Physical properties of the UD bio-based composites

As mentioned before, two violin soundboards, called S_1 and S_2, were manufactured for this study. Their physical properties are given in Table 1. It lists the values of the specific gravity, the fibre volume fraction and the porosity of the composite material.

Table 1: Specific gravity, fibre and void volume fraction for the two manufactured arched plates.

	S_1	S_2
Specific gravity	1.28	1.29
V_{fibre} (%)	64	58
V_{poro} (%)	3	2.2

The specific gravity is between 1.28 and 1.29 which is in agreement with the technical data-sheet of the material provider. The fibre volume fraction varies from 64 % to 58 % for S_1 and S_2, respectively. This significant variation is attributed to the slight variations in the parameters adjusted and applied during the manufacturing process (in particular, the preheating duration, the time from which the pressure was applied and the heating/cooling rate). The void volume fraction is in a range between 2.2 % and 3 %. Based on these physical properties and the ROM (described in the material and methods section), the longitudinal and transverse moduli of the composite material were estimated for each soundboard and given in Table 5. As mentioned earlier in the text, based on the provider data-sheet and data from the literature, the elastic modulus of

the matrix is considered to be equal to 3.5 GPa and the longitudinal and transverse moduli of the flax fibres are 60 GPa and 7 GPa, respectively. Using these values, the longitudinal modulus of the resulting composite material was evaluated to be equal to 41.4 and 36.6 GPa for the soundboards S_1 and S_2 respectively. In the transverse direction the elastic modulus was estimated to 5.5 and 5.1 GPa for S_1 and S_2.

3.2. Characterization of the UD bio-based composite using quasi-static tests

3.2.1. Longitudinal direction

Rectangular specimens were cut from the remaining flat parts of the arched plates used to make the soundboard S_1. They were used to determine the flexural properties of the composite material using 3-points bending tests. The results obtained in the longitudinal direction are shown in Fig. 4.

On the Fig. 4 (a), the stress is plotted as a function of the maximum bending strain. The scattering between the three different tested beam specimens is small. The curves show a non linear behaviour with a yield point somewhere between 0.5 and 1 % of strain. This is the typical behaviour of plant fibre composites. The average stress at failure is between 310 and 340 MPa, and the maximum strain at failure ranges from 1.9 and 2.2 %. These values are in agreement with those specified in the technical data-sheet of the flaxtape material, indicating a maximum strength and failure strain of respectively 294 MPa and 2.6 % for a 12 layers laminate processed by RTM with a fibre volume fraction of 50 %. These slight discrepancies can be attributed to both the difference in the fibre volume fraction and to the manufacturing process. The evolution of the apparent tangent modulus in the longitudinal direction as a function of the strain is plotted in Fig. 4 (b). The apparent modulus decreases as the strain increases. At 1 % strain, the apparent modulus is reduced by a factor of four as compared to the value at 0 % strain. As a consequence, we propose in this work to evaluate this modulus in a similar and reduced strain domain (at a theoretical value of 0 % strain) in order to compare results in a reliable manner. This apparent tangent and initial modulus is denoted $E^0_{L_{exp}}$. The average value, L_{avg}, displayed in the Table 2 is equal to 39.6 ± 0.9 GPa. This value is consistent with the technical data of the supplier giving a flexural modulus of 31 GPa for a fibre volume fraction of 50 % and consistent with the value of 41.4 GPa estimated using the rule of mixtures for a fibre volume fraction equal to 64 %.

3.2.2. Transverse direction

The Fig. 5 (a) represents the stress as a function of strain in the transverse direction. As expected for a unidirectional composite, in the transverse direction, the stress at failure is approximately one order of magnitude lower than for the longitudinal direction with a value ranging between 27 and 31 MPa. The maximum strain at failure is generally a little bit lower than 1 %. This premature failure in the transverse direction (when compared to the neat epoxy polymer) was attributed to a limited strength and initial defects at the interface between the flax fibre bundles and the epoxy matrix. The evolution of the apparent tangent modulus as a function of increasing strain is also given in Fig. 5 (b). As expected for this type of material, the apparent modulus decreases with increasing strain. The values of the transverse modulus at 0 % strain, $E^0_{T_{exp}}$, are given in Table 2. The average value T_{avg} is equal to 3.46 ± 0.16 GPa. This value is significantly lower than the one estimated by the ROM (i.e. 5.3 GPa). However, the transverse modulus is generally overestimated using the ROM, since it hypothesizes a perfect adhesion at the interface between the fibres and the matrix, which is hardly achieved from an experimental point of view. The prediction is also highly dependent to the properties of the constituents and it is well known that the transverse properties of the plant fibres are hard to be determined. The value used in this paper (7 GPa) is estimated from data in the literature and thus must be considered as questionable.

Table 2: Modulus of elasticity determined from quasi-static tests for longitudinal and transverse specimens, the values are given for 0% of strain.

	L_1	L_2	L_3	L_{avg}	T_1	T_2	T_3	T_{avg}
E^0_{exp} (GPa)	40.9	39.7	38.2	39.6	3.45	3.7	3.24	3.46

3.3. Characterization of the UD bio-based composite using DMA

A rectangular specimen, L_1, cut in the arched plate S_1 was also submitted to a dynamic mechanical analysis. Fig. 6 shows the evolution of the storage modulus E' and the loss factor $tan\delta$ of the material in the longitudinal direction as a function of the frequency. As expected for the considered temperature range, the storage modulus decreases with increasing temperature. The influence of the temperature on the storage modulus and the loss factor between -40 °C and 60 °C is relatively weak for the considered frequencies. The loss factor value ranges between 2 % and 4% up to 60 °C. At 20 °C, the loss factor is equal to 2.5 % for a test frequency of 1 Hz. This value is close to the one obtained in [31], where the loss factor in the longitudinal direction ranges between 1.7 % in a dry state and 2.7 % in a water vapour saturated state. The glass transition temperature (T_g) of the flax-epoxy composite is in a range between 75 and 90 °C. The glass transition temperature is lower than the one given by the supplier for the neat epoxy resin cured in the same condition (i.e. 130 °C). The T_g of the composite can differ from that of the neat epoxy matrix because it is sensitive to interfacial interactions between resin and reinforcements [32], and the presence of fibres can modify the motion of polymer chains. A slightly lower T_g was observed for natural fibre polypropylene composites compared to the pure PP by [33]. [34] attributed such difference to the polymer bond to the fibres that could result in a layer with properties different from the bulk properties of the pure polymer. In the case of the bio-based composite studied in this work, the shift in temperature at the scale of the composite when compared to the neat resin is more than 40 °C, and further experiments may be conducted to explain this shift. The T_g of the flax-epoxy composite is translated by a sharp decrease in the storage modulus that is sensitive to the excitation frequency. For the highest test frequency (4.6 Hz), the storage modulus decreases from 30 to 25 GPa. The decrease of the

Figure 4: Three-point bending mechanical characterization in longitudinal direction, (a): stress as a function of strain, (b): apparent modulus as a function of strain.

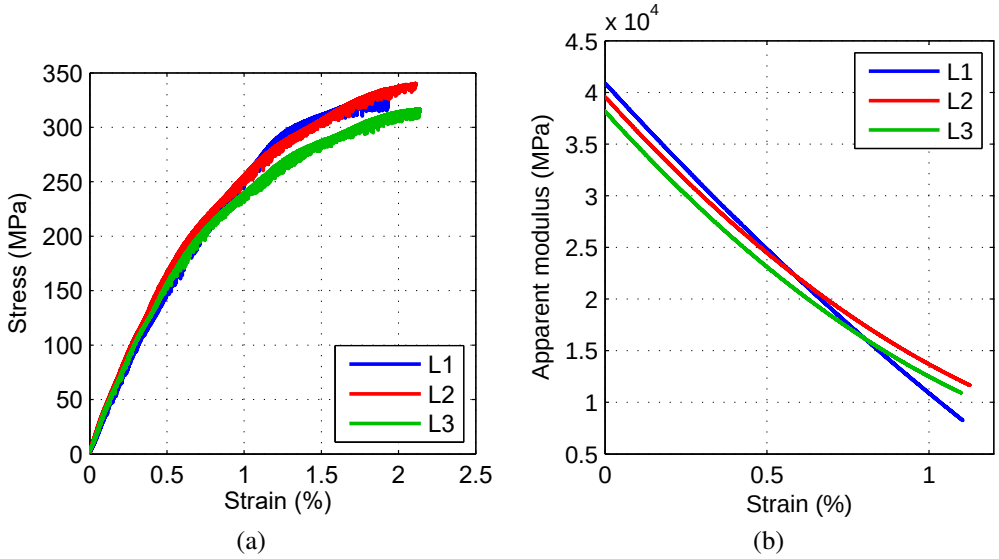

(a) (b)

Figure 5: Three-point bending mechanical characterization in transverse direction, (a): stress as a function of strain, (b): apparent modulus as a function of strain.

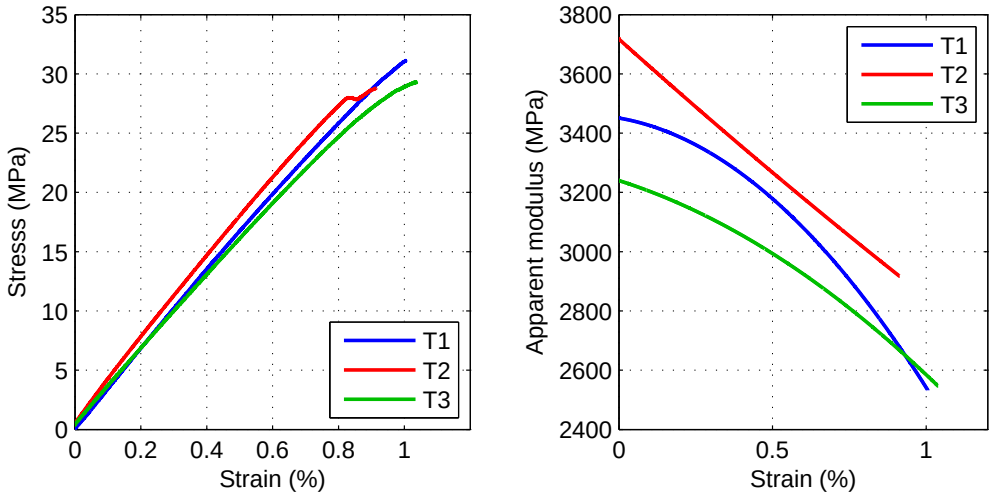

(a) (b)

storage modulus at the lowest test frequency (0.1 Hz) ranges from 28 to 20 GPa, which demonstrates a high impact of the frequency in this temperature domain. In this domain, the loss factor value reaches a peak whose value ranges between 10 and 12 % depending on the frequency. The master curve obtained at 24 °C is given in Fig. 7. The master curve is obtained with a model based on the time-temperature superposition (TTS) principle. The shift factors a_T used for the processing of the master curve are given as a function of the temperature in Fig. 8. The master curve gives the evolution of the storage modulus and loss factor as a function of a broader frequency range. The storage modulus increases with the frequency from approximately 15 GPa at a very low reduced frequency (10^{-10} Hz) to approximately 34 GPa at 1 Hz. This last value is consistent with the results obtained from the quasi-static tests, the elastic modulus being generally underestimated when using DMA tests. The prediction using the TTS principle also points out that the loss factor value reaches a maximum value at a reduced frequency equal to 10^{-7} Hz. It decreases from this point to a minimum value of approximately 2.3 % above a reduced frequency equal to 10 Hz, which is below the starting frequency of the FEMU-3DVF method. The bandwidth of the FEMU-3DVF method ranges between 100 and 2000 Hz. The values obtained with the FEMU-3DVF method, that are detailed below, are represented with the blue and black lines in Fig. 7.

3.4. Sensitivity analysis

A preliminary sensitivity analysis was performed. Results of the finite difference sensitivity analysis are displayed as a sensitivity matrix and are shown in Fig. 9 (a).

The numerical model of the soundboard and the experimental set-up were used to determine the parameter sensitivity and

Figure 6: Storage modulus and loss factor as a function of temperature for uni-directional composite in the longitudinal direction.

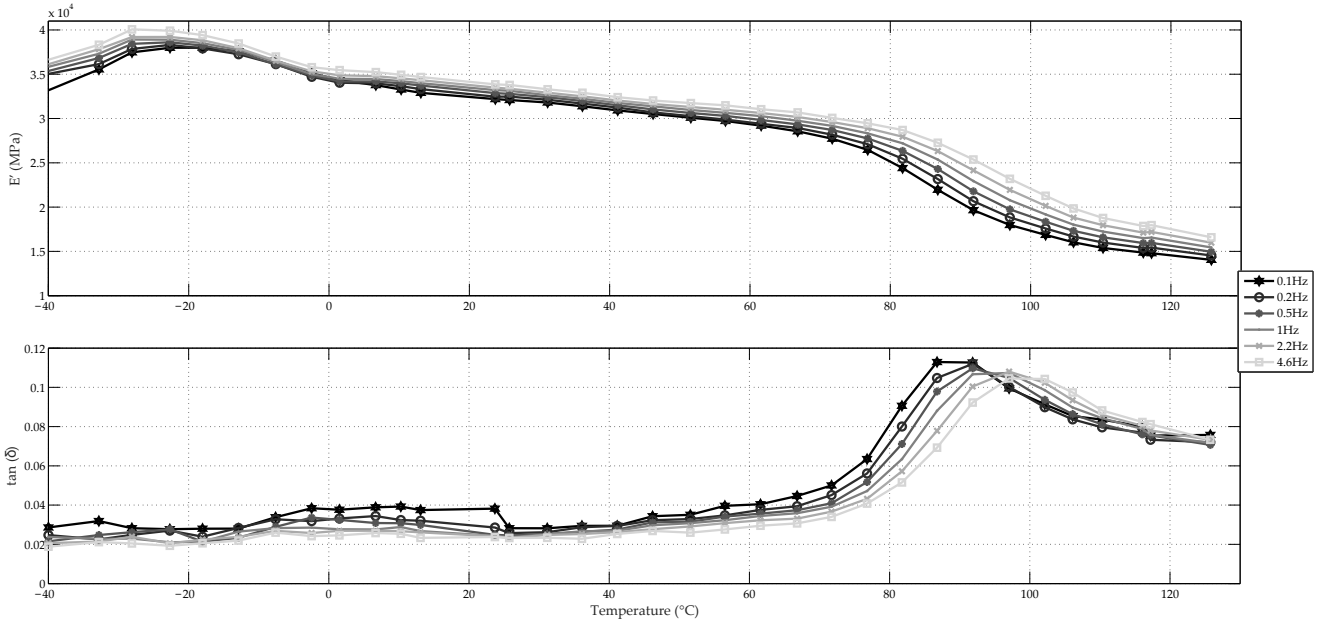

thus the parameters that would be identifiable in the considered experimental configuration. The obtained sensitivity matrix shows the sensitivity of each material parameter as a function of the considered mode. This matrix points out that three constitutive elastic properties (E_L, E_T and G_{LT}) mainly drive the dynamical behaviour of the soundboards for the given modes and in the studied frequency bandwidth. Similarly, based on this sensitivity analysis, the three loss factors η_L, η_T and η_{LT} are assumed to be reliably evaluated. The results of the Morris sensitivity analysis are shown in Fig. 9 (b). This global sensitivity analysis ranks the material parameters as a function of their influence on the vibratory behaviour of the soundboard for the 7 first modes. The shear modulus G_{LT} is mainly influential. The influence of the Young's moduli E_L and E_T is comparable. ν_{TL} is weakly influential, and the remaining parameters ν_{LT}, ν_{TT} and G_{TT} are not displayed since their influence on the dynamical response (in the considered experimental configuration) is too small. This means that they cannot be identified reliably. For this reason, their value will be fixed later in the development of the FEMU-3DVF method. A previous global sensitivity analysis made on a full violin [35] has also highlighted the fact that the dynamical behaviour of the soundboard is mainly driven by the same material parameters.

3.5. Characterization of the bio-based composite using FEMU-3DVF method

The two soundboards (S_1 and S_2) were finally characterized using the FEMU-3DVF method. The following subsections present the different steps and results obtained using this method.

3.5.1. Vibrational data

The frequencies of each mode for the two tested soundboards are given in Table 3.

Table 3: Eigenfrequencies of the two soundboard determined by LSCF modal analysis.

Mode	1	2	3	4	5	6
F_{S_1} (Hz)	221.4	476.9	620.5	776.4	835.1	1032.9
F_{S_2} (Hz)	217.0	466.75	623.1	/	808.1	1026.1

The eigenfrequencies of a part are dependent on its density, rigidities and dimensions. Thus, the discrepancies in the values of the eigenfrequencies can be attributed to the slight difference in the dimensions (the thicknesses range between 1.9 and 2.1 mm) and shape of the soundboards but also to their physical and constitutive elastic and damping properties. The Fig. 10 (a) represents some of the experimental and numerical modes of the soundboard S_1 selected among the seven matched modes. The shapes of these different modes are represented using a color scale where the blue color represents the minimum value and the red color the maximum value. This qualitative comparison shows similar patterns for the four deformed shapes displayed. The minimum and maximum displacement lines obtained at the scale of both experimental and numerical modes are consistent. As a quantitative approach, the MAC value is used and displayed in Fig. 10 (b). It represents the MAC matrix between experimental and numerical data for the specimen S_1 after the minimization process used with the FEMU-3VF method.

The MAC values are globally very high (above 0.8) which indicates very similar mode shapes between experimental and numerical data.

3.5.2. Mechanical properties of composite soundboards identified using FEMU-3DVF

As a result of the sensitivity analysis, the parameters ν_{TL}, ν_{LT}, ν_{TT} and G_{TT} were fixed during the parameter identification process. They were fixed at values of 0.065, 0.35, 0.3 for

Figure 7: Master curve for bio-based composite obtained by DMA, T_{ref}=24 °C.

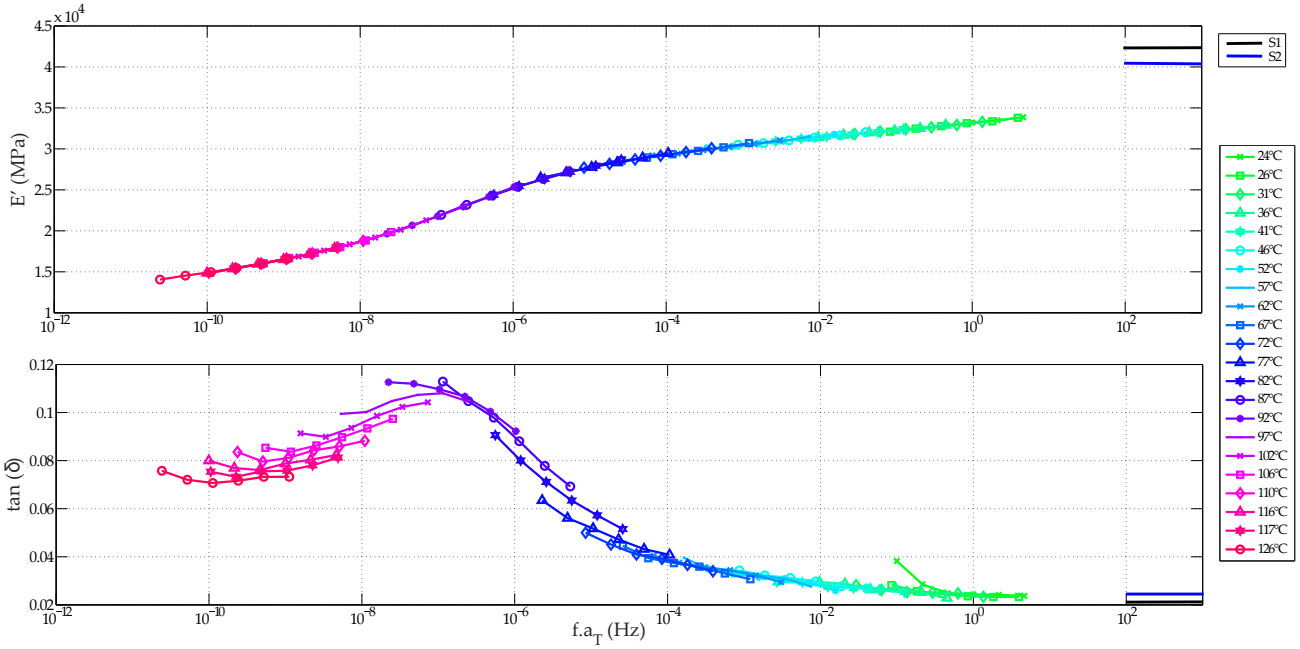

the Poisson's ratios ν_{TL}, ν_{LT}, ν_{TT}, respectively and 1.5 GPa for the shear modulus in the TT plane. It is also important to notice that the numerical models were built using the measured dimensions of the soundboards. The initial values of parameters to be identified were fixed at a value of 3.5±1.5, 40.0±10 and 2.3±0.6 GPa for E_T, E_L and G_{LT}, respectively. The averaged matched eigenfrequencies absolute error (MEE) and MAC values before and after the calibration are shown in Table 4.

Table 4: Mean matched eigenfrequencies error before (b.c.) and after (a.c.) calibration for the two soundboards, calculated with the eight first matched modes.

	S_1	S_2
Mean MEE b.c. (%)	2.2	5.9
Mean MAC b.c. (%)	87	88.1
Mean MEE a.c. (%)	0.5	0.85
Mean MAC a.c. (%)	87.2	87

The MEE decreases after the minimization process. Before the calibration, the averaged MEE is equal to 2.2 % for S_1 and 5.9 % for S_2. This indicates a correct matching of the numerical model with the initial parameters. After calibration, the mean MEE is equal to 0.5 and 0.85 % for S_1 and S_2 respectively, which indicates a good agreement between the numerical and experimental eigenfrequencies. The MAC value is close to 87 % which is an indicator of a correct matching between the two modal basis. As a reminder, the minimum criterion for the matching of the modes was set to 70 %.

3.5.3. Constitutive elastic properties

The mechanical properties identified are given in Table 5 which gives the longitudinal, transverse and shear moduli. The elastic moduli values are 38.3 and 34.9 GPa for E_L, 4.2 and 3.67 GPa for E_T and 2.3 and 2.0 GPa for G_{LT} for S_1 and S_2, respectively. These values are compared with the values evaluated with the ROM. The elasticity modulus in longitudinal direction, E_L, is lower for the samples S_1 (-7.5 %) and S_2 (-4.6 %). In the transverse direction, the differences are -23.6 % for S_1 and -28 % for S_2. The discrepancy between the identified values and the one evaluated with the ROM in the transverse direction is high. This can be explained in the same way as was explained in section 3.2.2, by the ROM strong hypothesis and uncertainty on the transverse elasticity of the flax fibres and their specific gravity. The identified value of E_L (38.3 GPa) for the sample S_1 is close to the averaged value of $E^0_{L_{exp}}$ (39.6 GPa) determined using the quasi-static flexural tests on the rectangular samples cut in the arched plate S_1. The identified value of E_T (4.1 GPa) is higher than the averaged value of $E^0_{T_{exp}}$ (3.46 GPa). This difference can be due, at least in part, to the difference in the excitation frequency between quasi-static tests and FEMU-3DVF. It can also be emphasized that in the FEMU-3DVF approach, the identified value results from a combination of different response modes, as well as different frequencies and the identified values are averaged in regard to the bandwidth of the vibrational method [200 Hz - 2000 Hz]. The master curve built from the DMA measurements (where T_{ref}=24 °C) gives a projection of the storage modulus at a frequency higher than 1 Hz. In DMA, the value of $E_{L_{DMA}}$ was evaluated at a strain level that is higher than for the FEMU-3DVF method. This can also explain, at least partly, the discrepancy between these two values. The storage modulus measured at room temperature and 1 Hz is equal to 34 GPa. The projection using the mastercurve of the storage modulus estimates its value at 37 GPa in the band between 100 and 1000 Hz.

Figure 8: Shift factors a_T as a function of the temperature.

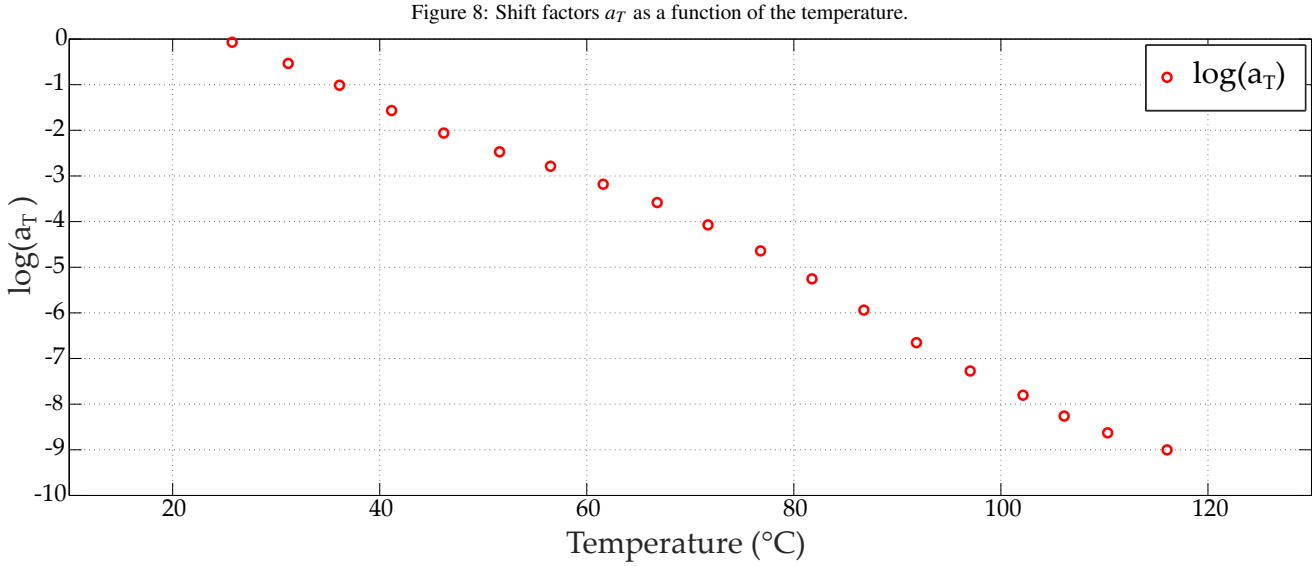

Figure 9: (a): sensitivity matrix for each material parameter as a function of the considered mode with finite differences sensitivity analysis, (b): ranking of the 4 main influential material parameters.

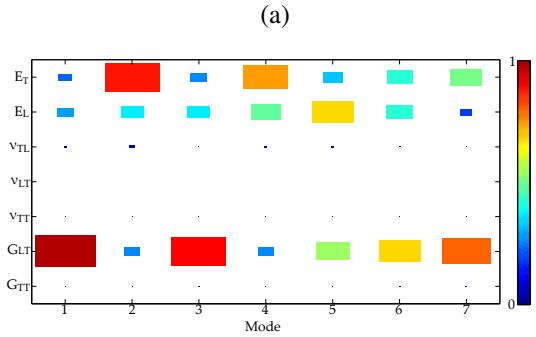

3.5.4. Constitutive damping properties

The loss factors evaluated using the FEMU-3DVF method are shown in Table 5.

Their values range between 2.2 and 2.4 % in L direction (η_L), and both values are equal to 2.4 % in LT plane ($\eta_{G_{LT}}$). In the transverse direction, the evaluated loss factor (η_T) is equal to 2.4 % for both samples. The values of η_L are in agreement with the DMA tests. For the arched plate S_1, the loss factor in the longitudinal direction is measured at a value of 2.3 %, using the DMA, which is in accordance with the value of 2.2 % obtained with the FEMU-3DVF method. As a comparison, the wood traditionally used to make soundboards, spruce (*Picea Abies*), exhibits in the similar material directions different damping capacities under standard conditions for temperature and relative humidity. The values of the loss factors of spruce are generally close to 0.7, 1.4 and 2.0 % in longitudinal (L), radial (R) and LR directions [36], respectively.

Table 5: Identified and measured values for bio-based composite.

		E_L (GPa)	E_T (GPa)	G_{LT} (GPa)	η_L (%)	η_T (%)	$\eta_{G_{LT}}$ (%)
ROM	S_1	41.4	5.5	/	/	/	/
	S_2	36.6	5.1	/	/	/	/
QS	Avg.	39.6	3.46	/	/	/	/
DMA	L_1	34	/	/	2.3	/	/
FEMU-3DVF	S_1	38.3	4.2	2.3	2.2	2.4	2.2
	S_2	34.9	3.67	2.03	2.4	2.4	2.4

3.5.5. Error quantification

Both direct and indirect methods deal with uncertainties in the evaluation (direct methods) or identification (indirect methods) of the parameters values. This section aims to evaluate the error in the identified values using FEMU-3DVF. A comparison is proposed between this indirect method and the quasi-static method used. The error of the FEMU-3DVF method can be related to the error made on the evaluation of the density, on the measurement of the dimensions (especially the thickness) and also related to the minimization algorithm (which can involve compensation effects or local minima). Table 6 gives the values of the error due to each source of uncertainty for each identified parameter on the sample S_1.

The error related to the measurement of the density is evaluated to be equal to 0.5 % of its value. This error leads to an error in the matched eigenfrequencies of the models of ± 0.45 %. This error leads to changes in the identified values using the minimization process of ± 1.3 % for E_L, ± 1.7 % for E_T and ± 0.9 % for G_{LT}. The error in the measurements of the dimen-

Figure 10: (a): examples of experimental (left) and numerical (right) modal deformed shapes, (b): MAC matrix between numerical and experimental modal basis after minimization procedure.

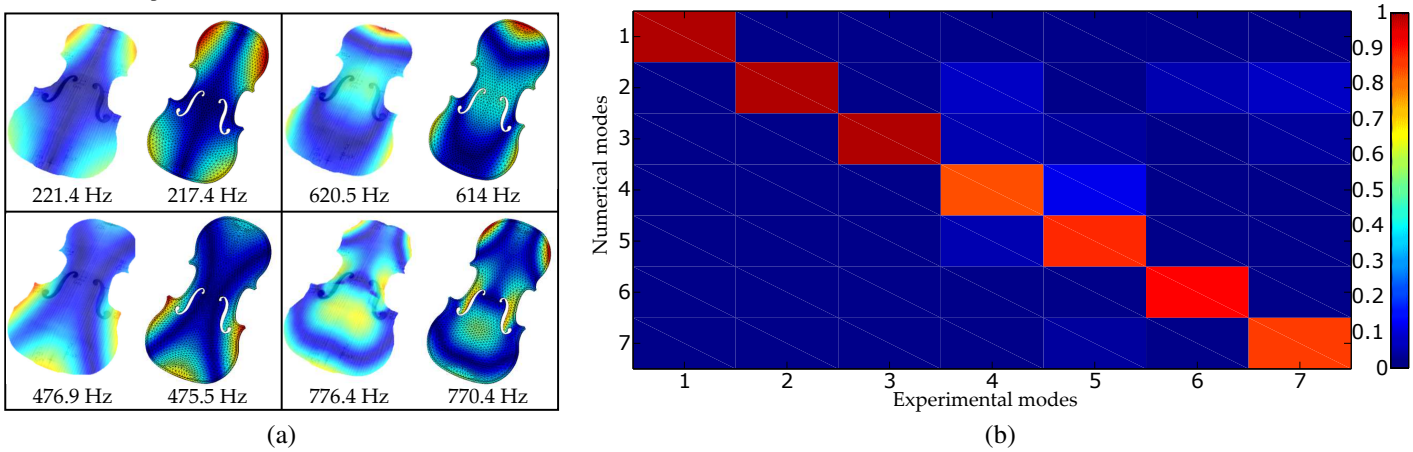

(a) (b)

Table 6: Evaluation of the relative error on the identified values of the parameters for different sources of error and uncertainties for the sample S_1.

	E_L	E_T	G_{LT}
Specific gravity error (%)	1.3	1.7	0.9
Thickness error (%)	2	6	4.3
Minimization error (%)	2.6	0.8	1.9

sions ($\pm$2.5 %) leads to relative errors in the eigenfrequencies of $\pm$2.5 %. This error leads to an error in the identified values of $\pm$2 % for E_L, $\pm$6% for E_T and $\pm$4.3 % for G_{LT}. The error related to the minimization algorithm leads to a relative error of $\pm$2.6 % for E_L, $\pm$0.8 % for E_T and $\pm$1.9 % for G_{LT}. These different sources of errors lead to a total error that varies according to the different material parameters. The total error proposed for the identified material parameters using the FEMU-3DVF method corresponds to the worst case, where the errors taken separately are at their maximum. For this sample, it is estimated at $\pm$5.9 % for E_L, $\pm$8.5 % for E_T and $\pm$7.1 % for G_{LT}. The loss factor evaluation is performed on the modal basis, and the determination algorithm leads to an absolute error of $\pm$0.2 %. As a comparison, the error in the measured $E^0_{i_{exp}}$, due to the accuracy of the load cell, the motion sensor and the sliding calliper, is close to 2.5 %, which is globally three times lower than the error on the identified rigidities using the FEMU-3DVF method.

4. Conclusion

The main objective of this work was to evaluate the capabilities of an inverse method for the identification of the constitutive elastic and damping properties of complex shape parts made of bio-based composites. For this purpose, two half-scale violin soundboards made of flax fibre reinforced epoxy resin material were manufactured and tested using the FEMU-3DVF proposed method. Results showed that three rigidities, E_L, E_T and G_{LT} as well as the damping properties in these corresponding directions can be determined successfully. The identified parameters were compared to the properties determined on the same composite material by quasi-static and DMA tests. The two violin soundboards specimens exhibited different material properties that are linked to their manufacturing process and the variability of their constituents. The longitudinal and transverse Young's moduli values of the UD flax fibre composite are equal to 38.3 and 34.9 GPa and 4.2 and 3.67 GPa. The shear modulus values are equal to 2.3 and 2.0 GPa, respectively. The error on the identified values is estimated to range between 5.9 and 8.5 %. The loss factor in the longitudinal and transverse directions, η_L and η_T are equal to 2.3$\pm$0.2 % and 2.4 $\pm$0.2%, and η_{LT} to 2.3$\pm$0.2, respectively. The FEMU-3DVF is a non-destructive relevant method. The results obtained are particularly encouraging for the composite sector, where the material properties are dependent of the manufacturing and/or the forming process. This method proves useful to estimate several material parameters simultaneously, where traditional measurements methods are most of the time destructive and estimate one parameter at a time. This method is relevant in the case of homogeneous structure parts. Heterogenous materials have not been studied. Numerous perspectives can be discussed, such as the evaluation of the dependence of the identified constitutive properties to the frequency and strain level, as described in [37]. As the measurement protocol is contact-free, it can be performed through the glass panel of a climatic chamber to characterize the influence of the environment (relative humidity, temperature, ageing) on the constitutive material properties of thermohygroscopic materials (mostly originated from the biomass). Moreover, the very small disturbances applied to the material (nanostrains) can be an asset for the refinement of the behaviour laws of such materials. Another application proposed is the design of unusually shape parts to identify material properties that are usually hard to identify by traditional methods.

Acknowledgements

The authors acknowledge MM. DORDOR Emmanuel and TISSOT Vincent for their support in the realization of the

aluminium mould and Prof. THIBAUD Sébastien and Dr. MICHEL Gérard for their kind support in laser machining. The authors acknowledge also the contribution of Dr. BUTAUD Pauline for performing the post-processing of the DMA data. This work was supported by the Laboratory of Excellence ACTION through the program Investments for the Future managed by the National Agency for Research (references ANR-11-LABX-01-01).

References

[1] L. Bruno, G. Felice, L. Pagnotta, A. Poggialini, G. Stigliano, Elastic characterization of orthotropic plates of any shape via static testing, International Journal of Solids and Structures 45 (3-4) (2008) 908–920, ISSN 00207683, doi:10.1016/j.ijsolstr.2007.09.017.

[2] G. Geymonat, Identification of elastic parameters by displacement field measurement, Comptes Rendus Mecanique 330 (2002) 403–408.

[3] S. Avril, M. Bonnet, A.-S. S. Bretelle, M. Grédiac, F. Hild, P. Ienny, F. Latourte, D. Lemosse, S. Pagano, E. Pagnacco, F. Pierron, Overview of Identification Methods of Mechanical Parameters Based on Full-field Measurements, Experimental Mechanics 48 (4) (2008) 381–402, ISSN 0014-4851, doi:10.1007/s11340-008-9148-y.

[4] M. L. M. François, Vers une mesure non destructive de la qualité des bois de lutherie, Revue des Composites et des Matériaux Avancés 10 (2009) 261–279.

[5] R. Longo, T. Delaunay, D. Laux, M. El Mouridi, O. Arnould, E. Le Clézio, Wood elastic characterization from a single sample by resonant ultrasound spectroscopy, Ultrasonics 52 (8) (2012) 971–974, ISSN 0041624X, doi:10.1016/j.ultras.2012.08.006.

[6] R. Gonçalves, A. Trinca, D. Cerri, Comparison of Elastic Constants of Wood Determined by Ultrasonic Wave Propagation and Static Compression Testing, Wood and Fiber Science 43 (2007) (2011) 64–75, ISSN 07356161.

[7] J. E. Mottershead, M. Link, M. I. Friswell, The sensitivity method in finite element model updating: A tutorial, Mechanical Systems and Signal Processing 25 (7) (2011) 2275–2296, ISSN 08883270, doi:10.1016/j.ymssp.2010.10.012.

[8] H. Sol, Identification of anisotropic plate rigidities using free vibration data, Ph.D. thesis, Free University of Brussels (VUB), 1986.

[9] M. McIntyre, J. Woodhouse, On measuring the elastic and damping constants of orthotropic sheet materials, Acta Metallurgica 36 (6) (1988) 1397–1416, ISSN 00016160, doi:10.1016/0001-6160(88)90209-X.

[10] T. Lauwagie, W. Heylen, H. Sol, O. Van Der Biest, Validation of a vibration based identification procedure for layered materials., in: Proceedings of ISMA2004, ISBN 9073802822, 1325–1336, 2004.

[11] M. Rébillat, X. Boutillon, Measurement of relevant elastic and damping material properties in sandwich thick plates, Journal of Sound and Vibration 330 (25) (2011) 6098–6121, ISSN 0022460X, doi:10.1016/j.jsv.2011.07.015.

[12] M. Schwaar, T. Gmür, J. Frieden, Modal numerical-experimental identification method for characterising the elastic and damping properties in sandwich structures with a relatively stiff core, Composite Structures 94 (7) (2012) 2227–2236, ISSN 02638223, doi:10.1016/j.compstruct.2012.02.017.

[13] M. Matter, T. Gmür, J. Cugnoni, A. Schorderet, Identification of the elastic and damping properties in sandwich structures with a low core-to-skin stiffness ratio, Composite Structures 93 (2) (2011) 331–341, ISSN 02638223, doi:10.1016/j.compstruct.2010.09.009.

[14] B. S. Ohlsson, M. Perstorper, Elastic Wood Properties From Dynamic Tests and Computer Modeling, Journal of Structural Engineering 118 (10) (1993) 2677–2690.

[15] Z. Huang, C. Zang, M. I. Friswell, Parameter identification of a printed circuit board structure using model updating and scanning laser vibrometer measurements, Proceedings of the International Conference on Noise and Vibration Engineering ISMA 2014 (2014) 2671–2682.

[16] M. A. Pérez Martínez, P. Poletti, L. Gil Espert, Vibration Testing for the Evaluation of the Effects of Moisture Content on the In-Plane Elastic Constants of Wood Used in Musical Instruments, in: C. Vasques, J. Dias Rodrigues (Eds.), Vibration and Structural Acoustics Analysis, Springer Netherlands, Dordrecht, ISBN 978-94-007-1702-2, 978-94-007-1703-9, 21–57, 2011.

[17] J. Cunha, J. Piranda, Identification of Stiffness Properties of Composite Tubes from Dynamic Tests, Experimental Mechanics 40 (2) (2000) 211–218, ISSN 00144851.

[18] J. H. Tam, Z. C. Ong, Z. Ismail, B. C. Ang, S. Y. Khoo, Identification of material properties of composite materials using nondestructive vibrational evaluation approaches: A review, Mechanics of Advanced Materials and Structures 0 (0) (2016) 1–16, ISSN 1537-6494, doi:10.1080/15376494.2016.1196798.

[19] L. Mehrez, A. Doostan, D. Moens, D. Vandepitte, Stochastic identification of composite material properties from limited experimental databases, part I: Experimental database construction, Mechanical Systems and Signal Processing 27 (1) (2012) 471–483, ISSN 08883270, doi:10.1016/j.ymssp.2011.09.001.

[20] L. Mehrez, A. Doostan, D. Moens, D. Vandepitte, Stochastic identification of composite material properties from limited experimental databases, Part II: Uncertainty modelling, Mechanical Systems and Signal Processing 27 (1) (2012) 484–498, ISSN 08883270, doi:10.1016/j.ymssp.2011.09.001.

[21] K. Ege, J.-F. Caron, S. Marcadet, H. Martin, Remplacement de la table d'harmonie du violon par un sandwich balsa/fibre de lin., in: Journées Scientifiques et Techniques AMAC - Matériaux composites renforcés par des fibres végétales, Lorient, 2010.

[22] S. Phillips, L. Lessard, Application of natural fiber composites to musical instrument top plates, Journal of Composite Materials 46 (2) (2012) 145–154, ISSN 0021-9983, doi:10.1177/0021998311410497.

[23] D. U. Shah, P. J. Schubel, M. J. Clifford, Can flax replace E-glass in structural composites? A small wind turbine blade case study, Composites Part B: Engineering 52 (2013) 172–181, ISSN 13598368, doi:10.1016/j.compositesb.2013.04.027.

[24] F. Bensadoun, I. Verpoest, J. Baets, J. Müssig, N. Graupner, P. Davies, M. Gomina, A. Kervoelen, C. Baley, Impregnated fibre bundle test for natural fibres used in composites, Journal of Reinforced Plastics and Composites (2017) 0731684417695461ISSN 0731-6844, doi:10.1177/0731684417695461.

[25] C. Baley, Y. Perrot, F. Busnel, H. Guezenoc, P. Davies, Transverse tensile behaviour of unidirectional plies reinforced with flax fibres, Materials Letters 60 (24) (2006) 2984–2987, ISSN 0167577X, doi:10.1016/j.matlet.2006.02.028.

[26] M. Matter, T. Gmür, J. Cugnoni, A. Schorderet, Numerical-experimental identification of the elastic and damping properties in composite plates, Composite Structures 90 (2) (2009) 180–187, ISSN 02638223, doi:10.1016/j.compstruct.2009.03.001.

[27] M. Carfagni, E. Lenzi, M. Pierini, The loss factor as a measure of mechanical damping, in: Proceedings-spie the international society for optical engineering, vol. 1, SPIE INTERNATIONAL SOCIETY FOR OPTICAL, 284–580, 1998.

[28] M. D. Morris, Factorial Sampling Plans for Preliminary Computational Experiments, Technometrics 33 (2) (1991) 161–174, ISSN 0040-1706, doi:10.2307/1269043.

[29] R. J. Allemang, D. L. Brown, A correlation coefficient for modal vector analysis, First International Modal Analysis Conference (1982) 110–116.

[30] P. Butaud, V. Placet, J. Klesa, M. Ouisse, E. Foltête, X. Gabrion, Investigations on the frequency and temperature effects on mechanical properties of a shape memory polymer (Veriflex), Mechanics of Materials 87 (April) (2015) 50–60, ISSN 01676636, doi:10.1016/j.mechmat.2015.04.002.

[31] M. Berges, R. Léger, V. Placet, V. Person, S. Corn, X. Gabrion, J. Rousseau, E. Ramasso, P. Ienny, S. Fontaine, Influence of moisture uptake on the static, cyclic and dynamic behaviour of unidirectional flax fibre-reinforced epoxy laminates, Composites Part A: Applied Science and Manufacturing 88 (2016) 165–177, ISSN 1359835X, doi:10.1016/j.compositesa.2016.05.029.

[32] A. Warrier, A. Godara, O. Rochez, L. Mezzo, F. Luizi, L. Gorbatikh, S. V. Lomov, A. W. VanVuure, I. Verpoest, The effect of adding carbon nanotubes to glass/epoxy composites in the fibre sizing and/or the matrix, Composites Part A: Applied Science and Manufacturing 41 (4) (2010) 532–538, ISSN 1359835X, doi:10.1016/j.compositesa.2010.01.001, URL `http://dx.doi.org/10.1016/j.compositesa.2010.01.001`.

[33] M. Tajvidi, R. H. Falk, J. C. Hermanson, Effect of natural fibers on thermal and mechanical properties of natural fiber polypropylene composites studied by dynamic mechanical analysis, Journal of Applied Polymer Science 101 (6) (2006) 4341–4349, ISSN 00218995, doi: 10.1002/app.24289.

[34] L. A. Pothan, S. Thomas, Polarity parameters and dynamic mechanical behaviour of chemically modified banana fiber reinforced polyester composites, Composites Science and Technology 63 (9) (2003) 1231–1240, ISSN 02663538, doi:10.1016/S0266-3538(03)00092-7.

[35] R. Viala, V. Placet, S. Cogan, E. Foltete, Model-Based Effects Screening of Stringed Instruments, Conference Proceedings of the Society for Experimental Mechanics Series 3 (2015) 151–156, ISSN 21915652, doi: 10.1007/978-3-319-15224-0.

[36] I. Brémaud, J. Gril, B. Thibaut, Anisotropy of wood vibrational properties: Dependence on grain angle and review of literature data, Wood Science and Technology 45 (4) (2011) 735–754, ISSN 00437719, doi: 10.1007/s00226-010-0393-8.

[37] A. Moreau, Identification de propriétés viscoélastiques de matériaux polymères par mesures de champs de réponses en fréquences de structures, Ph.D. thesis, INSA Rouen, 2007.